



Eco-friendly design of alginate-coated hydroxyapatites for the effective removal of Rhodamine B dye from water: equilibrium, kinetics and thermodynamic study

Sonia Jebri^{a,*}, Salsabil Idoudi^b, José Maria da Fonte Ferreira^c, Ismail Khattech^b

^aLaboratory of Desalination and Valorization of Natural Water, Water Researches and Technologies Center, Technologic Park of BorjCedria, B.P. 273, Soliman 8020, Tunisia, email: sonia.jebri@gmail.com

^bMaterials Cristal Chemistry and Applied Thermodynamics Laboratory, Chemistry Department, LR15SE01, Université de Tunis El Manar, Faculty of Science, Tunis 2092, Tunisia, emails: idoudisalsabil@gmail.com (S. Idoudi), ismail.khattech@fst.utm.tn (I. Khattech)

^cDepartment of Materials and Ceramics Engineering, CICECO-Aveiro Institute of Materials, University of Aveiro, 3810-193 Aveiro, email: jmf@ua.pt

Received 15 July 2022; Accepted 28 November 2022

ABSTRACT

Hydroxyapatite-alginate composites with different biopolymer contents (0%, 10%, 25% and 50%) were prepared according to an eco-friendly process using low-cost precursors. The prepared materials were firstly subjected to characterizations by Fourier-transform infrared spectroscopy, X-ray diffraction, scanning electron microscopy coupled with energy-dispersive X-ray spectroscopy and physisorption of N₂ techniques. The composites were then tested as sorbents for Rhodamine B dye under different sets of experimental conditions, including initial pH, contact time, initial dye concentration and temperature. The aim was to investigate the effects of these parameters on the extent of dye removal and to understand the adsorption behaviour of the composites under various conditions. The dye adsorption equilibrium is reached after 20 min of contact for the unmodified hydroxyapatite, being attained within a few minutes for the composite samples. Moreover, the pseudo-second-order kinetics model was found to be suitable to describe the adsorption of dye onto the uncoated product, contrarily to the modified compounds for which the kinetic data could be better predicted by the pseudo-first-order model. The equilibrium data were analysed by different isotherm models, with the Freundlich model providing the best fit. The maximum adsorption capacity increased from 225.2 to 289.5 mg/g by the grafting effect, suggesting the potential use of these materials in wastewater treatment.

Keywords: Hydroxyapatite-alginate composites; Eco-friendly; Low-cost; Rhodamine B; Adsorption

1. Introduction

Pigments and dyes are widely applied in textile, plastics, paper, cosmetic, food, and pharmaceutical industries. However, a huge amount of water is needed for the cleaning and washing processes in the different dye-related activities. Discharged into the water systems, these coloured effluents may prevent the sunlight to cross the lower layers

and hence threatening the aquatic life and inducing an ecotoxic hazard related to bioaccumulation, which may eventually affect the human life via food chain. Most of these compounds contain aromatic rings in their structures, which make them non-biodegradable, carcinogenic, mutagenic for aquatic life and very harmful for human health [1–3]. Therefore, various remediation techniques have been investigated to treat the coloured wastewater effluents.

* Corresponding author.

These methods included membrane filtration, photocatalytic degradation, electrocoagulation, biological treatment and adsorption process [4–8]. Among them, adsorption was found to be the most appropriate for the remediation of dyes in wastewaters. Besides, different kinds of adsorbents were employed for this purpose such as activated carbon, clays and agricultural solid waste [2,3].

Recently, many research studies highlighted the great ability of apatitic calcium phosphates for toxic metal neutralization in aqueous systems [9–11]. However, there is a lack of literature survey dealing with the possible application of these compounds as sorbents for dyes.

Calcium hydroxyapatite, with the general chemical formula $\text{Ca}_{10}(\text{PO}_4)_6(\text{OH})_2$, labelled thereafter CaHAp, is a multi-function material involved in different fields including biomaterials, catalysis and environmental applications [12–14]. This mineral has the advantages of being very stable, non-toxic, and able to exchange positive or negative-charged ion species in aqueous systems [15–18]. Adsorption of complex molecules, such as proteins and dyes, has also been evoked in numerous research papers [19,20].

On the other hand, one of the most important challenges of material science is the manufacture of low-cost materials with high performances and through eco-friendly synthesis procedures. Indeed, for the viability of a given process, mainly for environmental purposes, costs must be minimized. From this point of view, our present study is devoted on the elaboration of CaHAp coated with alginate-biopolymer for environmental applications through a green synthesis process. The prepared samples were subjected to characterisations by X-ray diffraction (XRD), Fourier-transform infrared spectroscopy (FT-IR), physisorption of N_2 and scanning electron microscopy coupled with energy-dispersive X-ray spectroscopy (SEM-EDS) techniques.

The Rhodamine B (RhB) was selected to evaluate the ability of the prepared materials to trap cationic dyes in water. RhB is often used as a fluorescent tracer within water to decide the rate and bearing of stream and transport, as a staining fluorescent in biotechnology applications and it is also extensively used as textile dye. According to a recent study, RhB exerts toxic effects on living organisms when its concentration exceeds 140 $\mu\text{g/L}$ in freshwaters [21].

The adsorption was investigated in batch equilibrium process; experimental data were subjected to kinetics and isotherm modelling, whereas temperature-dependent adsorption data were analysed for thermodynamic parameters.

2. Materials and methods

2.1. Chemical products

Cationic RhB dye having the chemical formula $\text{C}_{28}\text{H}_{31}\text{ClN}_2\text{O}_3$ was purchased from Loba Chemie. A stock solution of RhB was prepared by dissolving the corresponding quantity of the dye in distilled water. Calcium carbonate CaCO_3 (99%) and orthophosphoric acid H_3PO_4 (85 wt.%) were supplied from Fluka and were used as starting reactants for the synthesis of CaHAp powder. All the chemicals used in this study are of analytical grade and they were used as received without any further purification.

2.2. Materials preparation

2.2.1. Hydroxyapatite

Calcium hydroxyapatite labelled as CaHAp was prepared in open glass reactor. For a given synthesis, 10 mL of H_3PO_4 (0.15 mol) was pumped, at the rate of 2 mL/min, into 100 mL of calcium carbonate suspension CaCO_3 (0.25 mol). The mixture was kept under stirring for 24 h at constant temperature (80°C) [22]. The expected reaction can be described as follows:



The precipitate was separated from the mother liquor by vacuum filtration, and then dried for 12 h at 100°C.

2.2.2. Alginate-modified hydroxyapatites

The modified samples of hydroxyapatite with various alginate (Alg) amounts were obtained by reacting 4.0 g of CaHAp powder with 0.4, 1.0 and 2.0 g of sodium alginate in aqueous medium. The mixture was stirred for 1 h at 50°C and thereafter dried at 100°C. The prepared samples were labelled as CaHAp-*n*Alg where '*n*' is the mass ratio of alginate biopolymer in the prepared composite (*n* = 10, 25 and 50 wt.%). The possible modes of interaction between (Alg) molecules and CaHAp surface are schematized in Fig. 1, and thereby cationic dye could interact with COO^- functional groups of the bio-polymer through electrostatic forces [23]:

2.3. Characterization techniques

X-ray diffraction (XRD) analysis was carried out on D8 ADVANCE Bruker diffractometer (Germany) equipped with copper anticathode tube, with the voltage and current setting at 40 kV and 40 mA, respectively. Data were collected within the 2θ range between 10° to 60° with a 2θ -scan step width of 0.01947° $2\theta/\text{s}$. The FT-IR were recorded on Thermo Scientific-IR200 (USA) spectrophotometer within the wavenumber range from 400–4,000 cm^{-1} . Morphological studies and semi quantitative elemental analysis were undertaken by scanning electron microscopy coupled with energy-dispersive X-ray spectroscopy (SEM-EDX) using ultra-high-resolution analytical electron microscope HR-FESEM Hitachi SU-70 apparatus (Japan). Surface characteristics were determined through the adsorption–desorption of nitrogen (N_2) at 77 K on the material surface by referring to BET-method, using Gemini V2.00 equipment (Micromeritics Instrument Corp) (USA). In the liquid phase, the changes in RhB dye concentrations were measured using UV-Vis spectrophotometer (UV-1800 Shimadzu, Japan) calibrated at $\lambda_{\text{max}} = 554 \text{ nm}$, in the dye concentration range of 0–6 mg/L with a correlation coefficient $R^2 = 0.9981$.

2.4. Experimental protocol

The adsorption essays were carried out through a batch equilibrium technique with an adsorbent dose of 1 g/L. The experiments consist in reacting 25 mg of the adsorbent

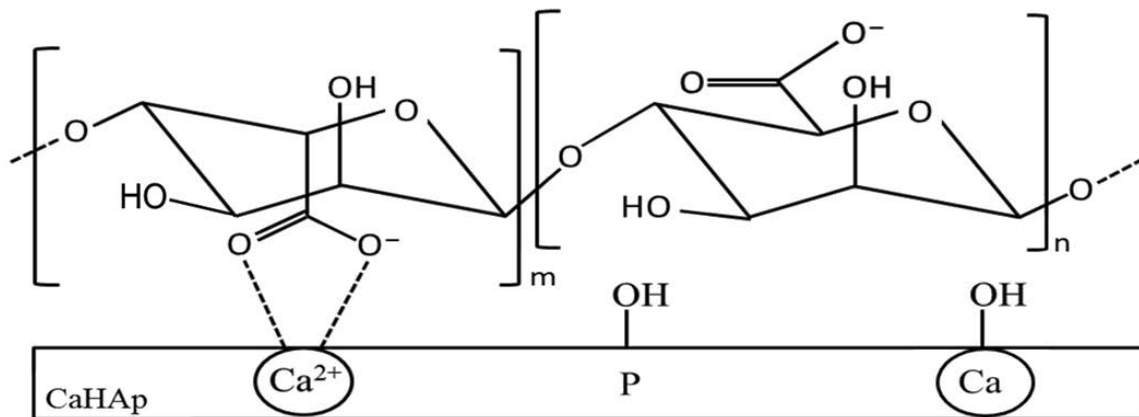


Fig. 1. Grafting of alginate biopolymer onto the CaHAp surface.

with 25 mL of the dye solution under various concentrations. The mixture was stirred for 1 h at 300 rpm and then sampled through vacuum filtration using a sintered glass. To study the effect of the acidity/alkalinity of the medium, the pH was varied within the range of 3–10 by dropwise additions of 0.1 M aqueous solutions of HCl or NaOH. The removal efficiency of dye (%) and the adsorption capacity q_t at any time t (mg/g) of the modified hydroxyapatites were calculated using Eqs. (1) and (2), respectively.

$$\text{Dye removal}(\%) = \frac{(C_0 - C_e)}{C_0} \times 100 \quad (1)$$

$$q_t = (C_0 - C_t) \times \frac{V}{m} \quad (2)$$

where C_0 and C_e are the dye concentrations (mg/L) in the liquid phase, initially and after the equilibration time, respectively. V is the solution volume (L), and m is the mass of the adsorbent powder (g). The experiments were carried out in duplicate and the performed data showed a standard deviation of less than 2%.

For the equilibrium and the kinetic studies, the non-linear regression analysis was applied using Microsoft Excel Solver [24]. The best fit for the experimental data was determined from the Chi-square test (χ^2) and the coefficient of determination (R^2). These functions are, respectively defined as:

$$\chi^2 = \sum_i^p \frac{(q_{\text{cal}} - q_{\text{exp}})^2}{q_{\text{cal}}} \quad (3)$$

$$r^2 = \frac{\sum_i^p (q_{\text{cal}} - q_{m,\text{exp}})^2}{\sum_i^p (q_{\text{cal}} - q_{m,\text{exp}})^2 + (q_{\text{cal}} - q_{m,\text{exp}})^2} \quad (4)$$

In these equations, q_{cal} and q_{exp} are respectively the calculated and the experimental data. $q_{m,\text{exp}}$ is the mean average values of the observed experimental data, and p is the number of experiments performed [24].

To evaluate the feasibility of using CaHAp-*n*Alg for successive adsorption–desorption cycles, the solid was stirred in alkaline medium using NaOH solution for 1 h after each cycle. The regenerated adsorbent was washed with deionized water several times to achieve neutral pH, dried at 70°C, and used for the next cycle.

3. Results and discussion

3.1. Characterization of adsorbents

3.1.1. FT-IR spectroscopy

The FT-IR spectra of the grafted and the uncoated CaHAp samples are shown in Fig. 2. They exhibit the features of PO_4^{3-} containing functional groups, which are located at 561, 577, 957 and 1,030 cm^{-1} , while the IR-band centred at 3,740 cm^{-1} is characteristic of the hydroxyl groups of the apatite structure [15]. Moreover, the broad bands observed towards 1,420 and 860 cm^{-1} are assigned to CO_3^{2-} groups. This may be explained by the incorporation of a few amounts of CO_3^{2-} group in the lattice due to the interaction between the formed free CaHAp and the carbon dioxide CO_2 resulted from the acid attack of the calcite during the synthesis step [22]. After surface modification, the intensity of the hydroxyl band decreases progressively with increasing Alg-grafting rate. This can be explained by the decrease in CaHAp fraction in the prepared composite. According to Fig. 1 (section 2.2.2), grafting of alginate biopolymer onto CaHAp surface can be made also through weak intermolecular interactions involving hydroxyl groups, and this is likely to contribute to a decreased intensity of the hydroxyl band. The spectra exhibit new vibration bands appearing at 1,410 and 1,600 cm^{-1} which are attributed to COO^- groups of Alg [23]. However, the intensity of these bands increases by the grafting rate. The grafting of alginate biopolymer onto CaHAp's surface through Ca^{2+} ions and the COO^- groups of Alg is, therefore, likely to contribute to this increasing intensity. Furthermore, the shift in the band position of COO^- groups present in the modified samples referring to their position in pure sodium alginate biopolymer could be explained by the establishment of $\equiv\text{CaOH}$ bonds with active sites of CaHAp [23].

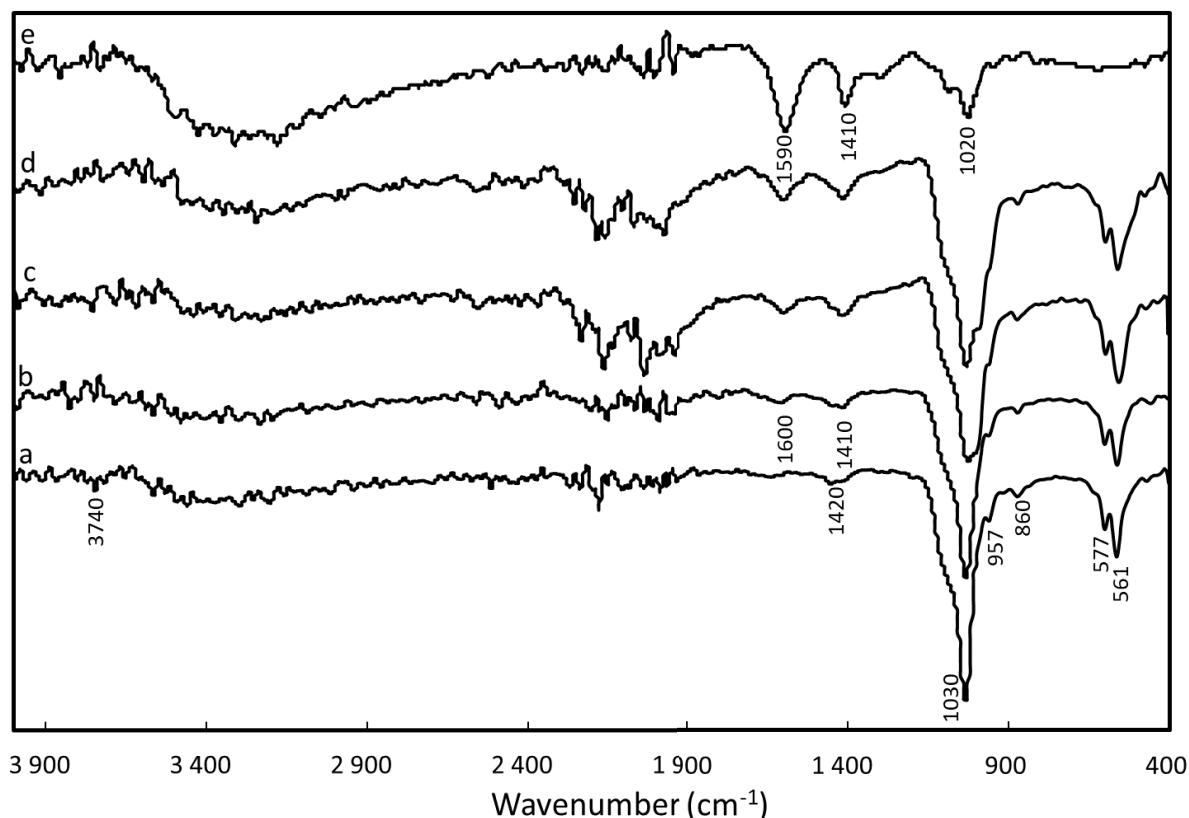


Fig. 2. Infrared spectra of: (a) initial CaHAp, (b) CaHAp-10%Alg, (c) CaHAp-25%Alg, (d) CaHAp-50%Alg and (e) alginate.

3.1.2. X-ray diffraction

XRD analysis was performed on the resulting products in order to identify the crystalline phases. The recorded patterns of the modified and the unmodified CaHAp samples are provided in Fig. 3. Thus, CaHAp is the main mineral calcium phosphate formed (JCPDS standard N°. 01-072-1243). On the other hand, the diffraction peak appearing at $2\theta = 29.4^\circ$ is related to calcium carbonate CaCO_3 (JCPDS standard N°. 00-047-1743). Indeed, the detection of this phase is not surprising and reveals the incomplete conversion of the initial calcite precursor to CaHAp during the precipitation process [22]. For all these samples, the crystallite sizes (D) were estimated from the Debye–Scherrer’s equation [25]:

$$D = \frac{k\lambda}{\beta_{hkl} \cos\theta_{hkl}} \quad (5)$$

where D is the crystallite size (nm); k is the shape factor, set to 0.9 for the apatite structure; λ is wavelength ($\lambda = 0.15406$ nm for Cu $K\alpha$ radiation); θ_{hkl} is the Bragg diffraction angle (in degrees) and β_{hkl} represents the broadening of the (hkl) diffraction peak measured at half of its maximum intensity (in radian). In this study, reflections (002) and (310) were selected to calculate the crystallite sizes D_{002} and D_{310} along the ‘ c ’ and ‘ a ’ axis, respectively. The calculated data reported in Table 1, suggest that the interaction between CaHAp and Alg-biopolymer has contributed to an apparent

decrease in crystallite size. This was unexpected, considering that the same starting CaHAp powder was used to prepare all the composite samples. Thus, an open question remains unanswered: is this just an apparent effect derived from the lower fraction of the CaHAp in the composites, or does the adsorption of Alg induces any real decrease in the crystallite size, or both? For nanometric particles, with a relatively high surface to volume ratio, the adsorption through crystalline forming ions is likely to enhance the apparent structural disorder.

The crystallinity degree of CaHAp (x_c) has been evaluated with respect to the alginate grafting level using to the following relationship [26]:

$$x_c = \left[\frac{k_A}{\beta_{002}} \right]^3 \quad (6)$$

where k_A is a constant parameter set to 0.24 and β_{002} is the full width at half maximum (FWHM) of the (002) reflection. The estimated values of x_c are listed in Table 1. Thus, increasing the grafted amount of the biopolymer onto the CaHAp surface reduced its crystallinity degree.

3.1.3. Textural properties

The surface features of CaHAp, both before and after modification with Alg-biopolymer, were determined through the BET method and the obtained data are collected

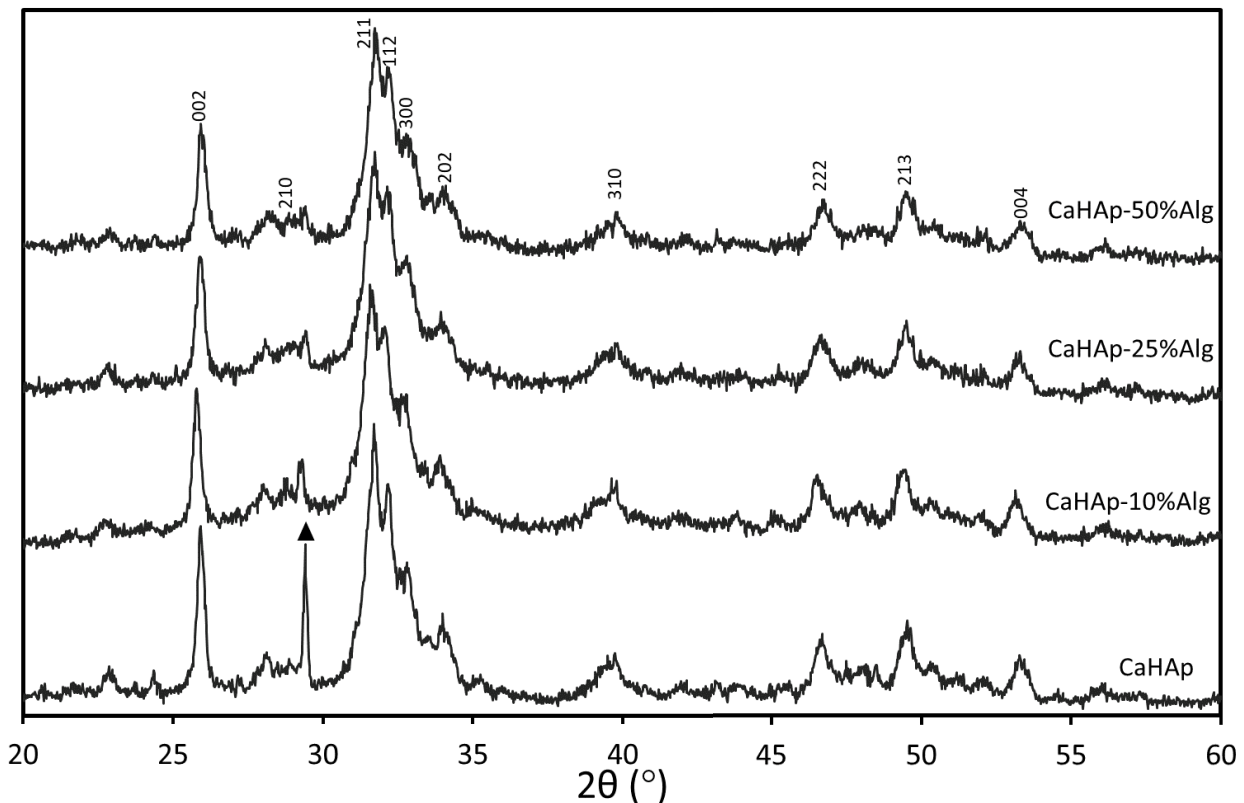


Fig. 3. XRD patterns of raw and modified hydroxyapatites; filled triangles calcite (JCPDS standard n° 00-47-1743); the other peaks CaHAp (JCPDS standard n° 01-072-1243).

Table 1
Crystallite sizes and crystallinity of CaHAp powders before and after alginate grafting

Sample	β_{002}	D_{002} (nm)	β_{310}	D_{310} (nm)	x_c
CaHAp	0.266	32.1	0.855	17.6	0.734
CaHAp-10%Alg	0.285	29.2	1.045	12.3	0.597
CaHAp-25%Alg	0.342	24.9	1.308	11.4	0.345
CaHAp-50%Alg	0.342	24.9	1.349	11.0	0.345

Table 2
Textural properties of CaHAp before and after Alg-biopolymer grafting

Sample	S_{BET} (m ² /g)	V_p (cm ³ /g)	D_p (Å)
CaHAp	41.5	1.036×10^{-1}	1.052×10^2
CaHAp-10%Alg	39.6	1.157×10^{-1}	1.174×10^2
CaHAp-25%Alg	28.4	8.835×10^{-2}	1.232×10^2
CaHAp-50%Alg	28.3	7.849×10^{-2}	1.084×10^2

in Table 2. Accordingly, the treatment of hydroxyapatite with alginate biopolymer promotes concomitant decreases in the surface area (S_{BET}) and in the total pore volume (V_p). These tendencies may be due to the filling of the internal and surface pores of initial hydroxyapatite with the biopolymer.

3.1.4. Morphological studies and elemental analysis

The morphological changes, induced on the surface of CaHAp after interaction with Alg-biopolymer, are shown in Fig. 4. The naked CaHAp particles exhibit irregular and poorly defined shapes with a low tendency to aggregate. The powder samples became strongly agglomerated upon alginate grafting, suggesting that the biopolymeric species adsorb onto the surfaces of neighbouring particles.

Based on EDS analysis (Fig. 4), Ca, P, O and C are the main elements of the grafted and the non-grafted samples. It is somewhat strange that the sample without Alg is the one with the most intense carbon peak. This is likely related to the presence of $CaCO_3$ in the final product as evinced by XRD studies and evoked in section 3.1.2.

3.2. Evaluation of the performances of CaHAp-Alg composites for the adsorption of RhB

3.2.1. pH dependence

Fig. 5 highlights the effect of acidity/alkalinity on the removal efficiency of RhB dye using CaHAp-Alg hybrid compounds at 298 K when the initial dye concentration is set to 5 mg/L. It is evident that the modified CaHAp samples exhibit higher efficiency in the removal of RhB dye

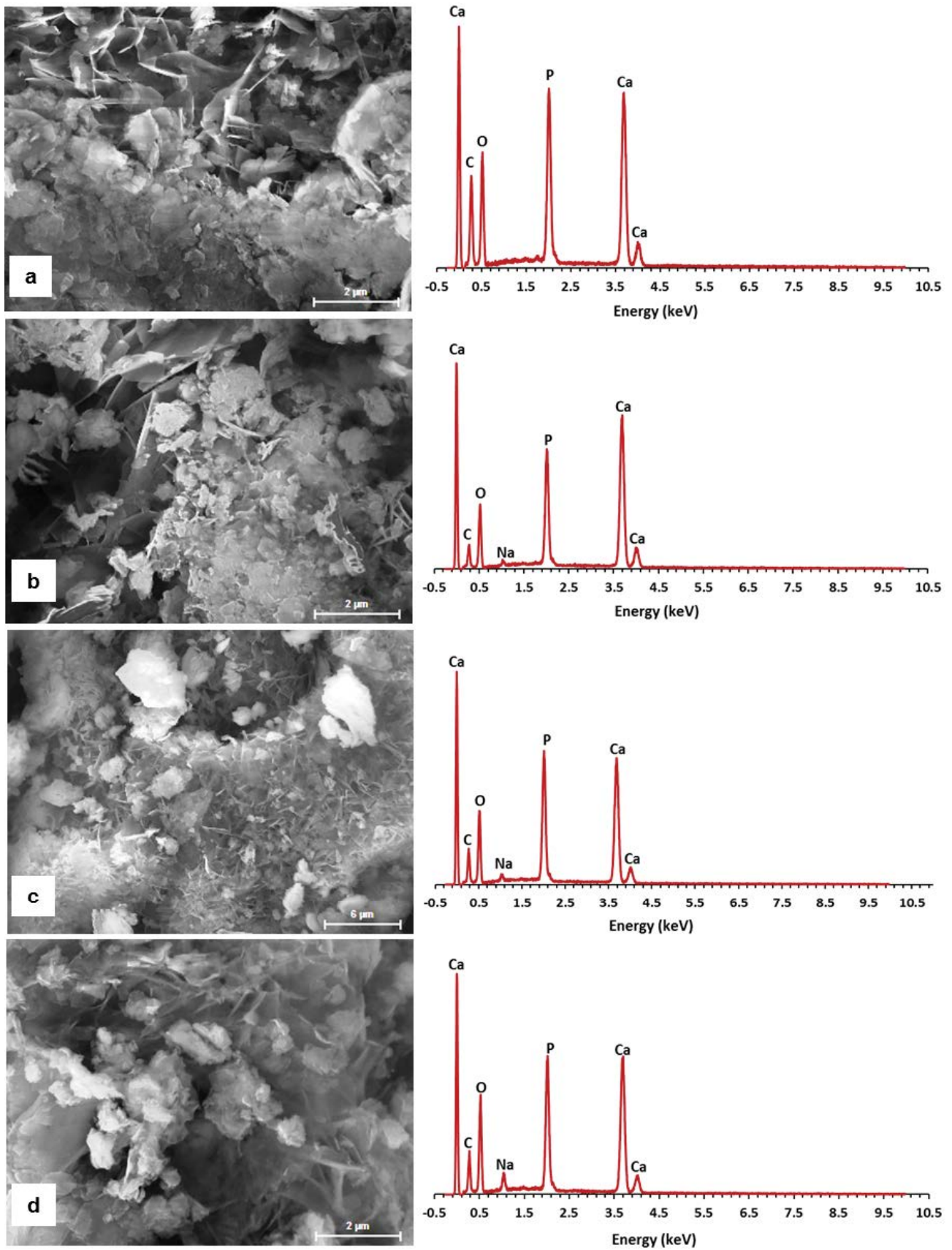


Fig. 4. SEM images and EDS spectra of: (a) initial CaHAp, (b) CaHAp-10%Alg, (c) CaHAp-25%Alg and (d) CaHAp-50%Alg.

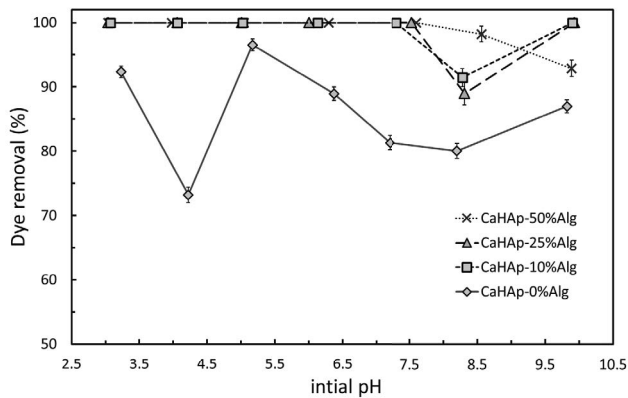


Fig. 5. Effect of the initial pH on the adsorption of RhB dye by CaHAp-*n*Alg compounds (*n* = 0%, 10%, 25% and 50%). Conditions: adsorbent dosage = 1 g/L, initial dye concentration = 5 mg/L, temperature = 297 K, contact time = 60 min.

compared to uncoated CaHAp. Indeed, the interaction between $-\text{COO}^-$ groups of alginate and the cationic dye enhanced the adsorption process. Furthermore, for the grafted samples, the results indicate that the adsorption is not pH-dependent when this parameter is set between 3 and 7. Otherwise, it is slightly reduced for higher pH values. This is not the case for the raw CaHAp, where the adsorption of dye is clearly affected by the pH. The maximum removal efficiency is observed at pH~5.5. Subsequently, no pH-adjustments were made for the grafted samples. However, this parameter was set to 5.5 for all experiments involving the unmodified CaHAp.

3.2.2. Effect of contact time

Fig. 6 shows the time-dependent evolution of the adsorption capacity of CaHAp-*n*Alg (with *n* = 0%, 10% and 50%) at 298 K when the initial dye concentration is set to 100 mg/L. It could be seen that the adsorption process was rapid in the first minute of contact, due to the availability of the high number of surface-active sites at the beginning of the phenomenon and then slowed down as time progresses. Hence, for CaHAp-0%Alg, the equilibrium extraction was approximately established after 20 min of contact, whereas, it could be reached within a few minutes for the grafted samples (CaHAp-10%Alg and CaHAp-50%Alg).

3.2.3. Effect of initial dye concentration

The effect of the initial dye concentration on removal of RhB dye using HAp-Alg hybrid compounds was investigated in the concentration range of 5–300 mg/L at 298 K. The results depicted in Fig. 7 indicate that, for all samples, near-complete recovery is observed when the initial dye concentration ranges from 5 to 50 mg/L. However, a decrease in the removal efficiency could be occurred for initial dye concentration exceeding 50 mg/L, especially for the materials with alginate ratio of 0%–10%. For the highly grafted samples (25% and 50%Alg), the reactivity with the cationic dye is slightly affected within the investigated concentration range.

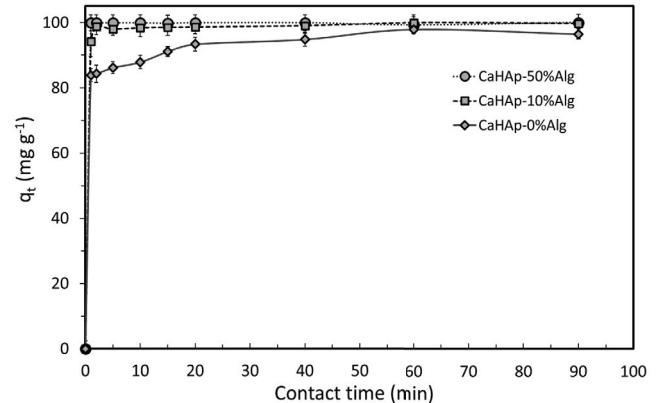


Fig. 6. Effect of the contact time on RhB adsorption by CaHAp-*n*Alg compounds with *n* = 0%, 10% and 50% (adsorbent dosage = 1 g/L, initial dye concentration = 100 mg/L, temperature = 298 K, pH~5.5).

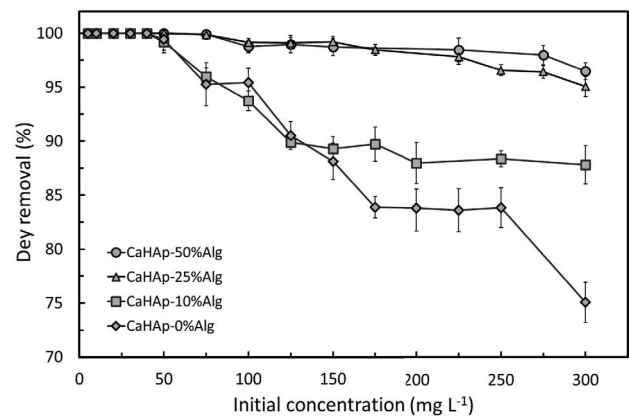


Fig. 7. Effect of initial RhB concentration on the removal efficiency of CaHAp-Alg hybrid compounds (adsorbent dosage = 1 g/L, temperature = 298 K, contact time = 60 min, pH~5.5).

In general, declining trends in the removal capacity may be related to the saturation of the active sites on the adsorbent surface that can occur in a highly concentrated medium.

3.2.4. Effect of temperature

The impact of temperature on the adsorption capacity of CaHAp-Alg compounds was investigated in the temperature range of 298–323 K. The experiments were carried out with an initial dye concentration of 100 mg/L. As shown in Fig. 8, the adsorption process was slightly affected by the increase of temperature for the highly grafted compounds (CaHAp-25%Alg and CaHAp-50%Alg), whereas, a significant decrease in the uptake capacity was observed for CaHAp and CaHAp-10%Alg. Meanwhile, the adsorption of RhB dye onto these samples is controlled by an exothermic process. This result agrees with a similar study devoted on the adsorption of Methylene blue dye onto hydroxyapatite-sodium alginate high-cost materials [23].

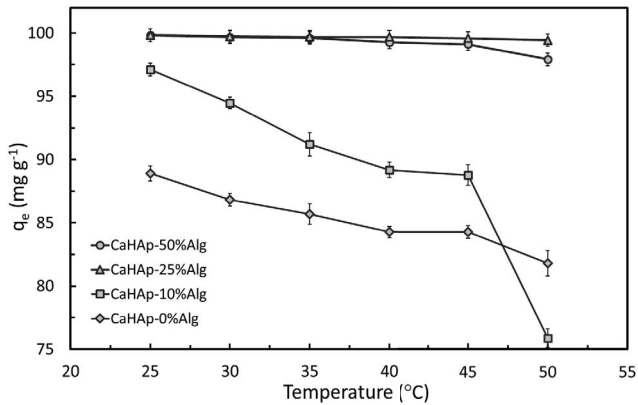


Fig. 8. Effect of temperature on the uptake of RhB dye by CaHAp-*n*Alg compounds (adsorbent dosage = 1 g/L, initial dye concentration = 100 mg/L, pH~5.5).

3.3. Adsorption kinetic modelling

The kinetic adsorption data were analysed using the Lagergren pseudo-first-order kinetic model, the pseudo-second-order, the Elovich and the intraparticle diffusion models.

The non-linear form of the pseudo-first-order and the pseudo-second-order kinetic models are, respectively, represented by the following equations [27,28]:

$$q_t = q_e (1 - e^{-k_1 t}) \quad (7)$$

$$q_t = \frac{k_2 q_e^2 t}{1 + k_2 q_e t} \quad (8)$$

where q_e and q_t are the amounts of dye sorbed at the equilibrium adsorption and at the contact time t , respectively (both in mg/g). k_1 and k_2 are the pseudo-first-order and pseudo-second-order sorption constants in (min^{-1}) and $\text{g}(\text{mg}/\text{min})$, respectively.

The applicability of the Elovich model for sorption kinetics was also examined using the non-linear form given by the following equation [29]:

$$q_t = \frac{1}{\beta} \ln(1 + \alpha \beta t) \quad (9)$$

where α [$\text{mg}(\text{g}\cdot\text{min})^{-1}$] is the initial adsorption rate and β (g/mg) a constant related to the extent of surface coverage and activation energy for chemisorption reactions.

Intraparticle diffusion was also explored. According to this model, the adsorbate species could be transported from the bulk of the solution into the solid phase through the intraparticle diffusion-transport process, which is often the rate-limiting step especially in a rapidly stirred batch reactor [30]. The non-linear form of the diffusion model is expressed as:

$$q_t = k_p t^{1/2} + C \quad (10)$$

where k_p is the intraparticle rate constant in ($\text{mg}(\text{g}\cdot\text{min})^{0.5}$) and C is a constant that provides an idea about the thickness of the boundary layer. According to this model, if the regression of q_t vs. $t^{1/2}$ is linear, but the plot does not pass through the origin, then the adsorption process involves intra-particle diffusion, but that is not the rate-limiting step.

The plot relative to the non-linear fits of pseudo-first-order, pseudo-second-order, Elovich and intraparticle diffusion kinetic models for the adsorption of RhB onto the selected CaHAp-Alg samples are presented in Fig. 9. The corresponding kinetic parameters are gathered in Table 3.

From Table 3, it can be seen that for the uncoated CaHAp, the non-linear form of the pseudo-second-order kinetic model seems to be more appropriate in adequately describing the adsorption process than the pseudo-second-order since it presents simultaneously a lower value of Chi-square (χ^2) and a very good coefficient of determination ($R^2 > 0.99$). Meanwhile, the adsorption phenomenon is well described by the pseudo-second-order kinetics model which is related to the chemical bonding reactions [28]. In this case, the initial adsorption rate h_2 [$\text{mg}(\text{g}\cdot\text{min})^{-1}$] can be expressed as $h_2 = k_2 q_e^2$ (Table 3). Increasing the grafting rate, the lowest Chi-square χ^2 values were observed for the pseudo-first kinetic model, suggesting a best prediction of the adsorption of RhB onto CaHAp-Alg compounds.

On the other hand, the data derived from the Elovich kinetic model were obtained with a good coefficient of determination R^2 and low Chi-square factor χ^2 . The results indicate a rise of the initial adsorption rate constant α with alginate grafting rate which supports the chemisorption interaction between the heterogeneous adsorbing and the molecules of RhB dye.

The plots of q_t vs. $t^{1/2}$ for the diffusion model show a relatively high correlation coefficient for the three selected adsorbents ($0.8955 \leq R^2 \leq 0.9487$) (results not shown), however, the straight lines did not intercept the origin, and thus intraparticle diffusion was assumed as not the only rate limiting step. The estimated value of the thickness of the boundary layer C increased with Alg-grafting rate.

3.4. Adsorption isotherms

The adsorption isotherms were applied to predict the type of interactions between adsorbent/adsorbate and to evaluate the maximum adsorption capacity at the equilibrium extraction. In this study, the equilibrium data were analysed with Langmuir, Freundlich, and Dubinin-Radushkevich isotherms models which are, respectively, expressed by Eqs. (11)–(13):

$$q_e = \frac{q_m k_L C_e}{1 + k_L C_e} \quad (11)$$

$$q_e = k_f C_e^{1/n} \quad (12)$$

$$C_{\text{ads}} = q_s \exp(-\beta \epsilon^2) \quad (13)$$

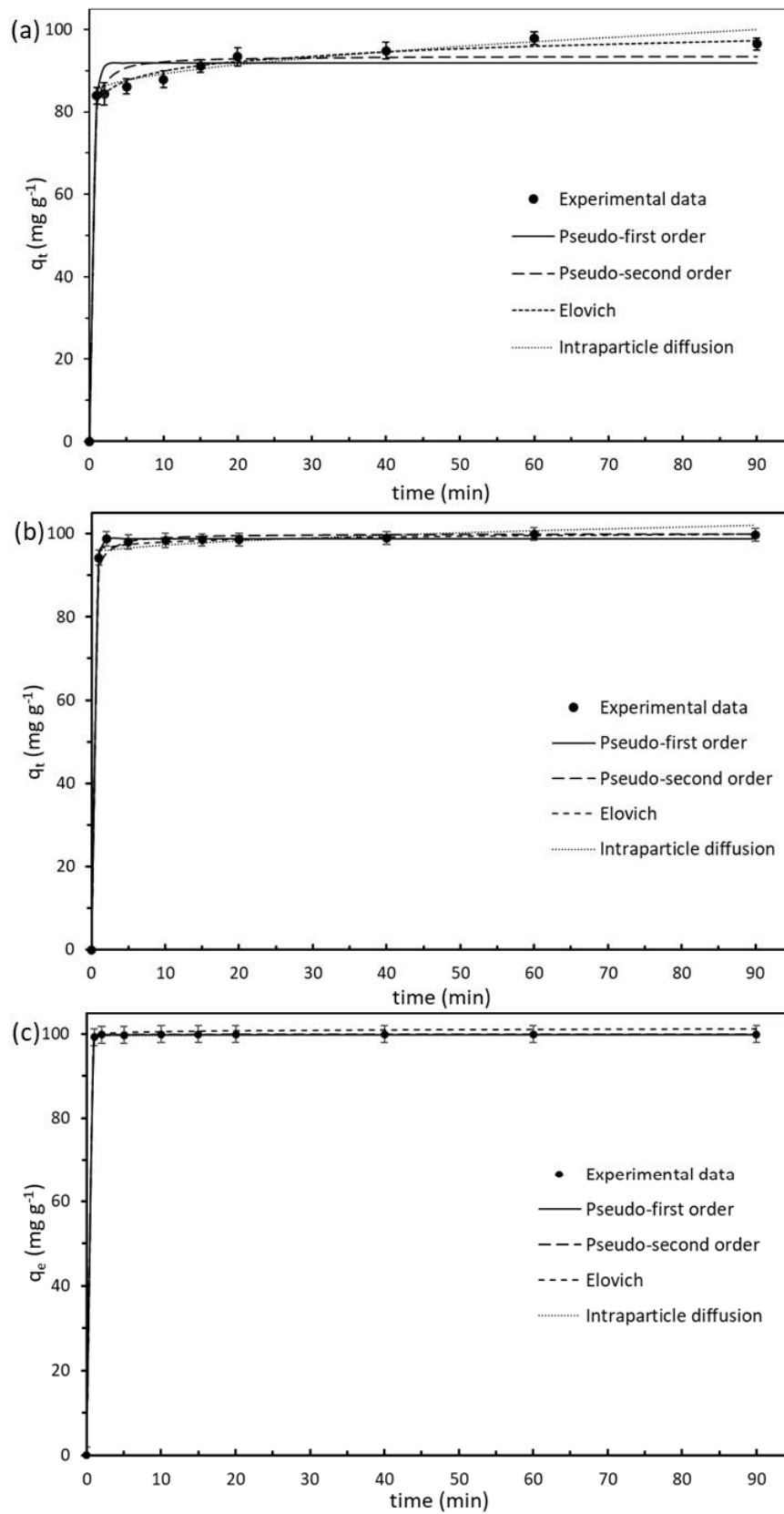


Fig. 9. Non-linear fits of pseudo-first-order, pseudo-second-order and Elovich kinetics for adsorption of RhB onto: (a) CaHAp, (b) CaHAp-10%Alg and (c) CaHAp-50%Alg.

Table 3
Kinetic data obtained by the non-linear fitting analysis of the adsorption of RhB onto CaHAp-Alg compounds

	CaHAp	CaHAp-10%Alg	CaHAp-50%Alg
$q_{e,exp}$ (mg/g)	97.2	98.8	99.8
Pseudo-first-order			
$q_{e,cal}$ (mg/g)	91.8	98.9	99.9
k_1 (min ⁻¹)	2.299	3.064	4.998
χ^2	1.7862	0.0311	0.0004
R^2	0.9838	0.9997	0.9999
Pseudo-second-order			
$q_{e,cal}$ (mg/g)	93.6	100.0	100.0
k_2 [g(mg·min) ⁻¹]	0.068	0.100	1.670
h_2 [mg(g·min) ⁻¹]	596.2	1,000	1.67×10^4
χ^2	0.9876	0.2762	0.0009
R^2	0.9911	0.9974	0.9999
Elovich model			
α [mg(g·min) ⁻¹]	1.38×10^{11}	1.67×10^{48}	9×10^{143}
β (g/mg)	0.297	1.158	3.333
χ^2	0.1675	0.0859	0.0541
R^2	0.9985	0.9991	0.9994
Intraparticle model			
k_p	1.7	0.75	0.05
C	83.9	95.0	99.6
χ^2	0.3049	0.1990	0.0023
R^2	0.9971	0.9980	0.9999

In Eq. (11), q_m (mg/g) and k_L (L/mg) are the Langmuir isotherm parameters related to the adsorption capacity and energy of adsorption, respectively. The separation factor R_L deduced from this model and expressed as $R_L = 1/(1 + k_L C_0)$ gives important information about the nature of the adsorption process. Thus, values of R_L indicate whether the adsorption is reversible ($R_L = 0$), favourable ($0 \leq R_L \leq 1$), linear ($R_L = 1$), or unfavourable ($R_L > 1$). In Eq. (12), k_f and n are the Freundlich isotherm parameters related to the adsorption capacity and intensity, respectively. In Eqs. (13), C_{ads} (mol/g) is the number of dye molecules adsorbed per unit mass of adsorbent and q_s (mol/g) is the theoretical saturation capacity. β (mol²/J²) is a coefficient related to the mean free energy of adsorption per mole of the adsorbate, and ε (J/mol) is the Polanyi potential expressed as: $\varepsilon = RT \ln(1 + 1/C_0)$, in which, R (J/mol·K) is the gas constant, and T (K) is the absolute temperature at the equilibrium experiment. The value of β constant provides an idea about the mean free energy E (kJ/mol), expressed as: $E = (2\beta)^{-0.5}$. The magnitude of apparent energy E is useful to estimate the type of adsorption. Thus, values of $E < 8$ kJ/mol suggest physical sorption, whereas values of E between 8 and 16 kJ/mol indicate that the adsorption process is described by ion exchange. For E values exceeding 16 kJ/mol, the adsorption occurs according to chemisorption process.

The Langmuir model assumes: (i) the formation of a monolayer onto the surface of the adsorbent with only one

being bonded adsorbate species on each adsorption site; (ii) the adsorbent surface is homogeneous in character, and the adsorption sites are identical and energetically equivalent. The Freundlich isotherm considers heterogeneous surfaces with a multilayer adsorption, whereas Dubinin–Radushkevich model is applicable to adsorption processes occurring on homogeneous and heterogeneous surfaces.

The adsorption isothermal studies were carried out at 25°C within the concentration range of 5–100 mg/L. The non-linear fits of the Langmuir, Freundlich and Dubinin–Radushkevich isotherm models for the adsorption of RhB dye onto CaHAp-Alg compounds are depicted in Fig. 10. The equilibrium parameters obtained by using the non-linear fits for the three selected models are given in Table 4.

Based on the results of Table 4, the estimated sorption capacity, q_m derived from the Langmuir model increased from ~240 to ~310 mg/g with the grafting rate. Besides, the R_L values are situated within the range of 0–1 for all samples, suggesting favourable adsorption of RhB dye onto HAp-Alg hybrid compounds under the current experimental conditions. The $1/n$ factor determined from the Freundlich isotherm model is within the range of 0.1–1, also confirming favourable conditions for the occurrence of the adsorption process. The values of mean free energy, E , derived from the Dubinin–Radushkevich isotherm model exceed 16 kJ/mol for the highly grafted

Table 4

Isotherm constants for the adsorption of RhB dye by CaHAp and CaHAp-Alg composites at $T = 298$ K, obtained by using the non-linear fits

Isotherm model	Adsorption constant	Adsorbent			
		CaHAp	CaHAp-10%Alg	CaHAp-25%Alg	CaHAp-50%Alg
Langmuir	q_{exp} (mg/g)	225.2	263.4	285.2	289.5
	q_m (mg/g)	239.8	240.0	283.0	310.0
	k_L (L/mg)	0.091	0.100	0.757	0.965
	R_L	0.444–0.013	0.411–0.011	0.104–0.002	0.102–0.002
	χ^2	332.7	222.5	146.0	247.2
	R^2	0.9403	0.9574	0.9812	0.9615
	k_f	51.7	60.00	133.7	143.0
Freundlich	n	2.89	2.79	3.50	3.52
	χ^2	16.0	37.4	3.2	37.3
	R^2	0.9608	0.9661	0.9868	0.9760
	q_s (mg/g)	528.2	772.4	879.6	816.3
Dubinin–Radushkevich	β (mol ² /J ²)	-1.99×10^{-9}	-2.40×10^{-10}	-1.73×10^{-10}	-1.68×10^{-10}
	E (kJ/mol)	15.8	14.4	17.1	17.2
	χ^2	22.2	49.6	5.6	50.5
	R^2	0.8884	0.8635	0.9848	0.8985

compounds suggesting a chemisorption reaction involving the establishment of chemical bonds between the modified adsorbent's surface and the adsorbate.

The overall comparison of the three isotherms indicates that the Freundlich isotherm remains the most appropriate in adequately describing the adsorption of RhB dye onto CaHAp-Alg compounds as evinced by the R^2 and χ^2 reliability factors. This isotherm does not predict any saturation of the sorbate, and thereby infinite surface coverage including multilayer adsorption is likely to occur.

Based on these findings, CaHAp's surface coating with alginate biopolymer improves its ability to trap dye molecules in water. The maximum absorption capacity ($q_{\text{exp}} = 289.5$ mg/g) was determined for the sample with 50% in Alg-content. This value has been compared to recently published data and the results are shown in Table 5. Accordingly, CaHAp-50%Alg exhibits the highest removal efficiency and therefore, was found to be suitable for remediating RhB dye from polluted waters.

3.5. Thermodynamic study on RhB dye sorption

The thermodynamic parameters relative to the adsorption of RhB dye onto CaHAp-Alg composites, such as standard Gibbs free energy (ΔG°), enthalpy change (ΔH°) and entropy change (ΔS°) were estimated by considering the following equations:

$$\Delta G^\circ = -RT \ln k_d \quad (14)$$

$$\Delta G^\circ = \Delta H^\circ - T\Delta S^\circ \quad (15)$$

$$\ln k_d = \frac{\Delta H^\circ}{RT} + \frac{\Delta S^\circ}{R} \quad (16)$$

Table 5

Literature data relative to the adsorption of RhB onto calcium phosphates and other adsorbents

Adsorbent	qe (mg/g)	Ref
CaHAp low-cost material	225.2	This work
CaHAp-Alg low-cost material	289.5	This work
CaHAp derived from animal bone meal	64.9	[31]
Commercial activated carbon	83–100	[32]
Beidellite-rich clay	268	[33]

where R is the gas constant (8.314 J/mol-K) and k_d is the distribution ratio of dye between the solid and the liquid phase expressed as: $k_d = q_e/C_e$.

The plot of $\ln(k_d)$ against $1/T$ for three selected samples CaHAp, CaHAp-10%Alg and CaHAp-50%Alg was linear in the range of the tested temperatures (Fig. 11). Thereby, the values of ΔH° and ΔS° were determined from the slope and the intercept of the plot and gathered in Table 6. The negative value of ΔS° indicated the decrease in randomness of the on-going process. Moreover, the absolute value of ΔH° is less than 40 kJ/mol in the case of the uncoated CaHAp, exceeding this quantity for the modified samples. These results indicate that physisorption is probably the dominating mechanism for the adsorption of RhB dye onto CaHAp, whereas the adsorption process is of chemical nature involving strong attraction forces for the functionalized samples.

3.6. Regeneration

CaHAp-50%Alg was selected for the regeneration essays since it was the most suitable one for the adsorption

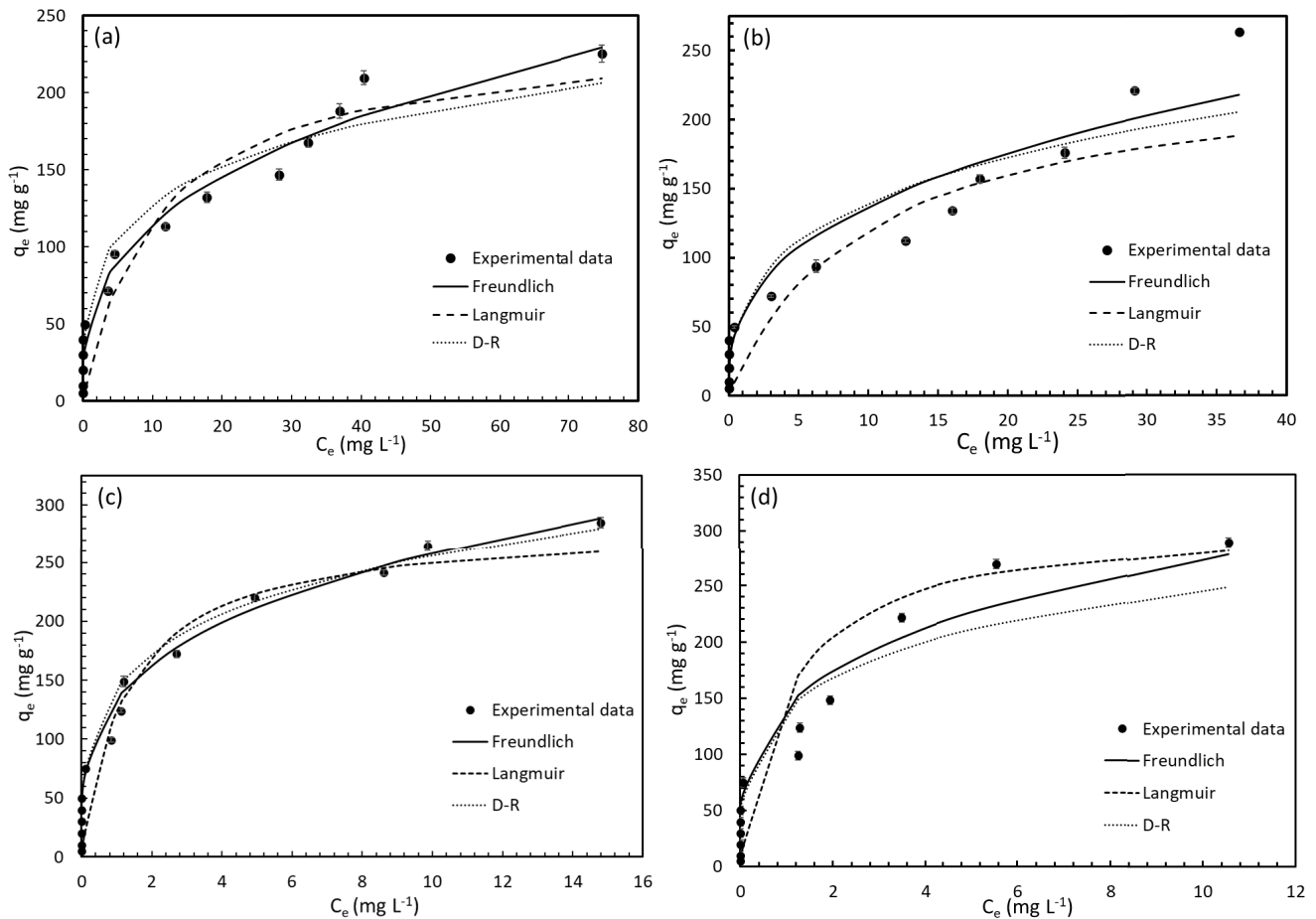


Fig. 10. Non-linear fits of the Langmuir, Freundlich and Dubinin–Radushkevich isotherm models for the adsorption of RhB dye onto: (a) CaHAp, (b) CaHAp-10%Alg, (c) CaHAp-25%Alg and (d) CaHAp-50%Alg (adsorbent dosage = 1 g/L, temperature = 298 K, pH~5.5).

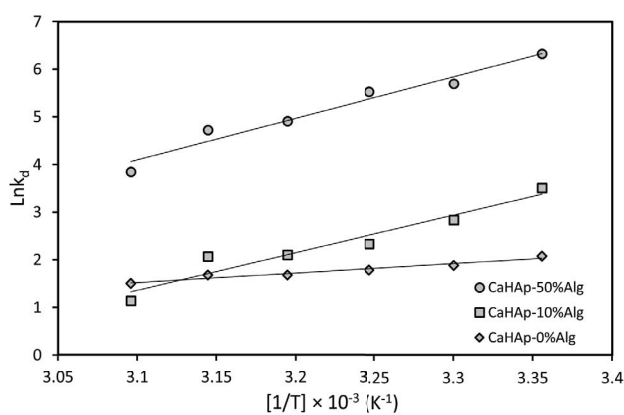


Fig. 11. Plot of $\ln k_d$ vs. $1/T$ for adsorption of RhB dye onto CaHAp- n Alg.

of RhB dye. The spent adsorbent was regenerated at 298 K, using NaOH solution at pH of 11.5 and then tested as a fresh adsorbent. For four cycles, the regeneration was achieved by batch desorption, and the results indicate that

the dye removal changed insignificantly after four regenerations. The RhB adsorption was still higher than 98%, indicating that CaHAp-50%Alg is highly reusable and exhibits high performance in RhB removal.

4. Conclusions

In this study, CaHAp was prepared at moderate conditions using calcium carbonate and orthophosphoric acid as convenient and low-cost starting precursors, and then, it was modified with different amounts of alginate biopolymer. These hybrid materials were designed to be conform to the actual tendency of green chemistry and synthesized at lab scale. However, considering the large volumes of wastewater needing remediation, it is critical to develop a cost-effective synthesis procedure capable to producing a large quantity of this high-quality powder for wastewater treatment on an industrial scale.

The characterizations of the hybrid compounds by FT-IR, XRD, physisorption of N_2 and SEM analysis confirm that the alginate was successfully grafted onto the CaHAp surface. The adsorption behaviour of these compounds towards RhB dye was investigated with respect to different

Table 6
Thermodynamic parameters for the adsorption of RhB onto CaHAp-Alg composites

Sample	ΔH°	ΔS°	ΔG° (kJ/mol)					
	(kJ/mol)	(J/K·mol)	298 K	303 K	308 K	313 K	318 K	323 K
CaHAp	-16.6	-38.7	-5.0	-4.8	-4.6	-4.5	-4.3	-4.1
CaHAp-10%Alg	-65.8	-192.6	-8.4	-7.4	-6.5	-5.5	-4.5	-3.6
CaHAp-50%Alg	-72.6	-191.0	-15.7	-14.7	-13.8	-12.8	-11.8	-10.9

parameters. Accordingly, the equilibrium adsorption was rapidly established suggesting their potential use as effective sorbent for this dye. On the other hand, the Freundlich model describes satisfactorily the adsorption process. This later does not predict any saturation of the adsorbent surface, and thereby infinite surface coverage including multilayer adsorption is likely to occur.

The adsorption capacities of CaHAp, CaHAp-10%Alg, CaHAp-25%Alg and CaHAp-50%Alg at equilibrium are respectively 225.2, 263.4, 285.2 and 289.5 mg/g. Meanwhile, such surface modification improved the reactivity of CaHAp towards the cationic dye. Based on the thermodynamic study, the dye adsorption process by hydroxyapatite hybrid compounds is exothermic in nature and driven by chemical interactions.

CaHAp-50%Alg's recoverability investigation, showed that about 98% of the removal rate can be retained after four regeneration cycles, suggesting its excellent recyclability and sustainability. Hence, CaHAp-50%Alg offers broad application prospects in the field of environmental restoration.

References

- R. Azmat, F. Bibi, Impacts of textile waste water on fingerlings of fresh water reservoir, *Asian J. Chem.*, 25 (2013) 9341–9344.
- S. Dutta, B. Gupta, S.K. Srivastava, A.K. Gupta, Recent advances on the removal of dyes from wastewater using various adsorbents: a critical review, *Mater. Adv.*, 2 (2021) 4497–4531.
- T. Robinson, G. MacMullan, R. Marchant, P. Nigam, Remediation of dyes textile effluent: critical review on current treatment technologies with a proposed alternative, *Bioresour. Technol.*, 77 (2001) 247–255.
- A.E. Abdelhamid, A.A. El-Sayed, A.M. Khalil, Polysulfone nanofiltration membranes enriched with functionalized graphene oxide for dye removal from wastewater, *J. Polym. Eng.*, 40 (2020) 833–841.
- S. Rajendran, M.M. Khan, F. Gracia, J. Qin, V.K. Gupta, S. Arumainathan, Ce³⁺-ion-induced visible-light photocatalytic degradation and electrochemical activity of ZnO/CeO₂ nanocomposite, *Sci. Rep.*, 6 (2016) 31641, doi: 10.1038/srep31641.
- A.I. Adeogun, R.B. Balakrishnan, Kinetics, isothermal and thermodynamics studies of electrocoagulation removal of basic dye Rhodamine B from aqueous solution using steel electrodes, *Appl. Water Sci.*, 7 (2017) 1711–1723.
- I.M. Banat, P. Nigam, D. Singh, R. Marchant, Microbial decolorization of textile dye containing effluents: a review, *Bioresour. Technol.*, 58 (1996) 217–227.
- H. El Boujaady, A. El Rhilassi, M. Bennani-Ziatni, R. El Hamri, A. Taitai, J.L. Lacout, Removal of a textile dye by adsorption on synthetic calcium phosphates, *Desalination*, 275 (2011) 10–16.
- R. Aouay, S. Jebri, A. Rebelo, J.M.F. Ferreira, I. Khattech, Enhanced cadmium removal from water by hydroxyapatite subjected to different thermal treatments, *J. Water Supply Res. Technol. AQUA*, 69 (2020) 678–692.
- S. Jebri, M. Jaouadi, I. Khattech, Precipitation of cadmium in water by the addition of phosphate solutions prepared from digested samples of waste animal bones, *Desal. Water Treat.*, 217 (2021) 253–261.
- S. Jebri, J.M.F. Ferreira, I. Khattech, Effective removal of heavy metals from water by apatitic tricalcium phosphate subjected to different thermal treatments, *Desal. Water Treat.*, 238 (2021) 207–217.
- C. Combes, C. Rey, Amorphous calcium phosphates: synthesis, properties and uses in biomaterials, *Acta Biomater.*, 6 (2010) 3362–3378.
- M. Achchar, C. Lamonier, A. Ezzamarty, M. Lakhdar, J. Leglise, E. Payen, New apatite-based supports prepared by industrial phosphoric acid for HDS catalyst synthesis, *C.R. Chim.*, 12 (2009) 677–682.
- M.P. Mahabole, R.C. Aiyer, C.V. Ramakrishna, B. Sreedhar, R.S. Khairnar, Synthesis, characterization and gas sensing property of hydroxyapatite ceramic, *Bull. Mater. Sci.*, 28 (2005) 535–545.
- S. Jebri, I. Khattech, M. Jemal, Standard enthalpy, entropy and Gibbs free energy of formation of "A" type carbonate phosphocalcium hydroxyapatites, *J. Chem. Thermodyn.*, 106 (2016) 84–94.
- S. Jebri, H. Boughzala, A. Bechrifa, M. Jemal, Structural analysis and thermochemistry of "A" type phosphostrontium carbonate hydroxyapatites, *J. Therm. Anal. Calorim.*, 107 (2012) 963–972.
- S. Jebri, A. Bechrifa, M. Jemal, Standard enthalpies of formation of "A" type carbonate phosphobarium hydroxyapatites, *J. Therm. Anal. Calorim.*, 109 (2012) 1059–1067.
- J.B. Slimen, M. Hidouri, M. Ghouma, E.B. Salem, S.V. Dorozhkin, Sintering of potassium doped hydroxy-fluorapatite bioceramics, *Coatings*, 11 (2021) 858, doi: 10.3390/coatings11070858.
- K. Wang, M. Wang, Q. Wang, X. Lu, X. Zhang, Computer simulation of proteins adsorption on hydroxyapatite surfaces with calcium phosphate ions, *J. Eur. Ceram. Soc.*, 37 (2017) 2509–2520.
- W. Lemlikchi, N. Drouiche, N. Belaicha, N. Oubagha, B. Baaziz, M.O. Mecherri, Kinetic study of the adsorption of textile dyes on synthetic hydroxyapatite in aqueous solution, *J. Ind. Eng. Chem.*, 32 (2015) 233–237.
- L.M. Skjolding, L. vG Jørgensen, K.S. Dyhr, C.J. Köppl, U.S. McKnight, P. Bauer-Gottwein, P. Mayer, P.L. Bjerg, A. Baun, Assessing the aquatic toxicity and environmental safety of tracer compounds Rhodamine B and Rhodamine WT, *Water Res.*, 197 (2021) 117109, doi: 10.1016/j.watres.2021.117109.
- D.P. Minh, S. Rio, P. Sharrock, H. Sebei, N. Lyczko, N.D. Tran, M. Raii, A. Nzihou, Hydroxyapatite starting from calcium carbonate and orthophosphoric acid: synthesis, characterization, and applications, *J. Mater. Sci.*, 49 (2014) 4261–4269.
- Y. Guesmi, H. Agougui, R. Lafi, M. Jabli, A. Hafiane, Synthesis of hydroxyapatite-sodium alginate via a co-precipitation technique for efficient adsorption of Methylene blue dye, *J. Mol. Liq.*, 249 (2018) 912–920.
- I.H.T. Kuete, D.R.T. Tchuifon, G.N. Ndifor-Angwafor, A.T. Kamdem, S.G. Anagho, Kinetic, isotherm and thermodynamic studies of the adsorption of thymol blue onto powdered activated carbons from garcinia cola nut shells impregnated with H₃PO₄ and KOH: non-linear regression analysis, *J. Encapsulation Adsorpt. Sci.*, 10 (2020) 1–27.

- [25] K. Venkateswarlu, A. Chandra Bose, N. Rameshbabu, X-ray peak broadening studies of nanocrystalline hydroxyapatite by Williamson–Hall analysis, *Physica B*, 405 (2010) 4256–4261.
- [26] K. Senthilarasan, A. Ragu, P. Sakthivel, Synthesis and characterization of hydroxyapatite and gelatin doped with magnesium chloride for bone tissue engineering, *Int. J. Eng. Res. Technol.*, 3 (2014) 917–921.
- [27] S. Lagergren, About the theory of so called adsorption of soluble substances, *K. Sven. Vetensk. Handl.*, 24 (1898) 1–39.
- [28] Y.S. Ho, Review of second-order models for adsorption systems, *J. Hazard. Mater.*, 136 (2006) 681–689.
- [29] S.H. Chien, W.R. Clayton, Application of Elovich equation to the kinetics of phosphate release and sorption in soils, *Soil Sci. Soc. Am. J.*, 44 (1980) 265–268.
- [30] T.W. Weber, R.K. Chakravoti, Pore and solid diffusion models for fixed-bed adsorbers, *AIChE J.*, 20 (1974) 228–238.
- [31] M. El Haddad, R. Mamouni, N. Saffaj, S. Lazar, Evaluation of performance of animal bone meal as a new low-cost adsorbent for the removal of a cationic dye Rhodamine B from aqueous solutions, *J. Saudi Chem. Soc.*, 20 (2016) S53–S59.
- [32] K. Jedynak, D. Wideł, N. Rędzia, Removal of Rhodamine B (A Basic Dye) and Acid Yellow 17 (An Acidic Dye) from aqueous solutions by ordered mesoporous carbon and commercial activated carbon, *Colloids Interfaces*, 30 (2019) 1–16.
- [33] H. Belhanafi, A. Bakhti, N. Benderdouche, Study of interactions between Rhodamine B and a Beidellite-rich clay fraction, *Clay Miner.*, 55 (2020) 194–202.